

INFLUENCE OF STRUCTURAL MODIFICATIONS ON THE AEROELASTIC ANALYSIS OF LARGE TRANSPORT AIRCRAFT

Balis Crema, L., Mastroddi, F.,
 Dip. Aerospaziale - Università degli Studi di Roma "La Sapienza"
 Via Eudossiana 16, 00184 Rome, Italy

Coppotelli, G., Iazzetta, A., Pecora, M.
 CIRA - Centro Italiano Ricerche Aerospaziali
 Via Maiorise, 81043, Capua (CE), Italy

Abstract

In the present paper an aeroelastic analysis on Ultra High Capacity Aircraft (*UHCA*) with emphasis on the aeroelastic sensitivities is performed. Because of the large flexibility of the wing structure of this kind of airplane, two flutter analysis recommended in the technical literature have been performed: the aileron reversal analysis and the wing flutter analysis in presence of the engine nacelle. The use of the finite-state modelling for the unsteady aerodynamics has allowed to carry out explicitly the aeroelastic sensitivity problem and then to predict locally the aeroelastic behavior as function of some design variables as the fuel weight, the wing stiffness, and the engine location. The numerical results are relative to the case of a *UHCA* wing with data provided by CIRA.

Introduction

The reduction of the direct operating costs has recently stimulated the interest on the new ultra high capacity aircraft. This evident advantage has as counterpart the increasing weight and flexibility of the wings with consequence on static and dynamic aeroelasticity, see Försching ^(1, 2, 3): specifically, bending deflection of the wing tip can reach almost 3-4 m with consequent reduction in effective angle of attack and the effectiveness of trailing-edge control surface. Furthermore, the loss of stiffness in the lifting surface, the mass distribution, and - above all - the positioning of the turbofan engines (with higher and higher by-pass ratio) can provide a reduction in the natural frequency and a consequent reduction in the flutter speed (*e.g.*, the first bending natural frequency can be less than 1

Hz and the first nacelle engine pitching frequency less than 2*Hz*, Försching ⁽²⁾): indeed, a root locus relative to an aeroelastic system exhibits as the lower modes are typically the critical ones in the flutter stability scenario, Bisplinghoff ⁽⁴⁾. The use of aeroelastic sensitivities, see Haftka ^(5, 6) either to structural parameters (mass or stiffness variations, thickness variations, etc.) or to configuration parameters (as the engine-nacelle positions) can be of great interest in the design of this kind of airplane where the aeroelastic constraints are to be carefully taken into account. Indeed, the typical flutter speeds must be expected to be close to the maximum cruising flight speeds.

The influence of the structural modifications in the aeroelastic stability analysis has been analyzed by Striz and Venkayya ⁽⁷⁾ where the influence between structural (finite element method) and aerodynamic (lifting surface method) discretization has been also investigated in the framework of the structural optimization with flutter constraints.

A lot of papers on the numerical methods for the numerical evaluation of the aeroelastic sensitivities (*e.g.*, Cardani and Mantegazza ⁽⁸⁾), for standard eigensensitivity formulae (*e.g.*, Rogers ⁽⁹⁾) are available in the technical literature. A relevant simplification on the sensitivity evaluation problem was obtained with the use of finite-state aerodynamics, Jones ⁽¹⁰⁾, Karpel ⁽¹¹⁾, Morino et al. ⁽¹²⁾: indeed, this advantage was shown in Karpel ^(13, 14) where also the influence of the modal variations for optimization problems in static and dynamic aeroelasticity was investigated.

In Balis Crema et al. ⁽¹⁵⁾ a study on the influence of the structural modification in the evaluation of the aeroelastic sensitivities was carried out: and the portion of Generalized Aerodynamic Force (GAF) matrix which is "structure-dependent" (*i.e.*, which is de-

pendent on the natural-vibration modes) was explicitly identified. This goal was reached considering the standard modal description for the structure, a compressible unsteady potential integral formulation for the aerodynamics (e.g., Morino ^(16, 17) or Albano et al. ⁽¹⁸⁾, Giesing et al. ⁽¹⁹⁾) and the finite-state aerodynamic approximation proposed Morino et al. ⁽²⁰⁾. These variations considered in the mentioned paper were not modifications in the lifting-body geometry but only on the vibrational characteristics: in the present paper the formulation for the sensitivity problem proposed by Balis Crema et al. ⁽¹⁵⁾ is used for the aeroelastic-sensitivity analysis of a *UHCA* but considering also the body shape variation due to the nacelle position or the diameter magnitude which is an essential issue for the aeroelastic performance of the high capacity aircraft.

In the next Section the basic aeroelastic model for the study of stability and the aileron reversal together with the finite-state aerodynamics formulation will be presented; next, the aeroelastic sensitivities formulation will be shown; finally, the numerical results and comments.

As apparent from Balis Crema et al. ⁽¹⁵⁾, the first three authors are responsible for the content of the Section entitled *Aeroelastic Sensitivities*, for that of the Section entitled *Numerical Results* concerning the aeroelastic sensitivity while the other authors are responsible of the remainders of the this Section. All the authors are responsible of the section entitled *Aeroelastic Model and Finite State Aerodynamics*.

Aeroelastic Model and Finite-State Aerodynamics

Consider an aeroelastic system described in terms of the amplitudes, $q_n(t)$ ($n = 1, \dots, N$), of the natural modes of vibration, $\phi^{(n)}$, which are here assumed to be normalized, so as to have the generalized masses equal one. The corresponding Lagrange equations of motion, neglecting structural damping and gravity, are given by, Bisplinghof ⁽⁴⁾,

$$\frac{d^2 \mathbf{q}}{dt^2} + \mathbf{\Omega}^2 \mathbf{q} = q_D \mathbf{f} \quad (1)$$

where $\mathbf{\Omega}$ is the diagonal matrix of the natural (angular) frequencies of vibration of the structure, $q_D = \rho_\infty U_\infty^2 / 2$ is the dynamic pressure, whereas the components of \mathbf{f} are the generalized aerodynamic forces associated with the n^{th} mode, $\phi^{(n)}$ ($n = 1, \dots, N$), as

$$q_D f_n = \iint_S \mathbf{t} \cdot \phi^{(n)} dS \quad (2)$$

where \mathbf{t} is the aerodynamic force per unit area acting on S . Here, we assume that the aerodynamic

forces depend linearly upon the Lagrangean coordinates $q_n(t)$; specifically, in the following we limit ourselves to potential subsonic or supersonic flows (the modeling of viscous effects, particularly important for the control surfaces, and/or of transonic effects, falls beyond the scope of the present paper). Hence, the Laplace transform of the generalized force vector can be expressed as (in the following the Laplace transform of a time dependent function $f(t)$ will be indicated as $\tilde{f}(s)$, where s is the Laplace variable)

$$\begin{aligned} \tilde{\mathbf{f}}(s) &= \tilde{\mathbf{f}}_m(s) + \tilde{\mathbf{f}}_a(s) \\ &= \mathbf{E} \left(\frac{sb}{U_\infty} \right) \tilde{\mathbf{q}}(s) + \mathbf{E}_\beta \left(\frac{sb}{U_\infty} \right) \tilde{\beta}(s) \end{aligned} \quad (3)$$

where $\tilde{\mathbf{f}}_m(s)$ are the aerodynamic forces due to the elastic motion and $\tilde{\mathbf{f}}_a(s)$ are those due to the control surface (e.g., the aileron motion) whereas \mathbf{E} and \mathbf{E}_β are the so-called aerodynamic matrices. As emphasized by Eq. 3, the aerodynamic matrices are function of s and U_∞ only through the variable $p := sb/U_\infty$, which is known as the complex reduced frequency (b is the reference semi-chord). Note that \mathbf{E} may be obtained analytically for some simple cases (e.g., classic Theodorsen incompressible 2-D aerodynamic theory); otherwise, $\mathbf{E}(p)$ and $\mathbf{E}(p)_\beta$ are evaluated numerically, for instance, by doublet-lattice (Giesing ⁽¹⁹⁾), or panel methods (Morino ^(21, 22)). More precisely, the algorithm for the evaluation of $\mathbf{E}(p)$ is typically available only along the imaginary axis: $\mathbf{E}(p)$ is then the analytic continuation of $\mathbf{E}(ik)$ being $k := \text{Imag}[p]$ the so-called reduced frequency.

In the case of compressible potential flow (Morino ⁽²²⁾ and Balis Crema et al ⁽¹⁵⁾), the GAF matrix is a $N \times N$ matrix which can be exactly decomposed in three contributions:

$$\mathbf{E}(p) = \mathbf{E}_C(p) \mathbf{E}_B(p) \mathbf{E}_A(p) \quad (4)$$

such that only $\mathbf{E}_C(p)$ and $\mathbf{E}_A(p)$ are explicitly dependent upon the assumed modes: in the same paper it was shown that the influence of the structural variation on these matrices are negligible and this issue has been emphasized in the results presented in this paper. Indeed, from the above equations the GAF matrix \mathbf{E}^* including the structural modifications is given by

$$\begin{aligned} \mathbf{E}^* &= \mathbf{E}_C^* \mathbf{E}_B \mathbf{E}_A^* = \mathbf{E}_C \mathbf{E}_B \mathbf{E}_A + \\ &+ \Delta \mathbf{E}_C \mathbf{E}_B \mathbf{E}_A + \mathbf{E}_C \mathbf{E}_B \Delta \mathbf{E}_A + \Delta \mathbf{E}_C \mathbf{E}_B \Delta \mathbf{E}_A \end{aligned} \quad (5)$$

As shown in Balis Crema et al. ⁽¹⁵⁾, in the Eq. 5 there are contributions of order $\Delta \phi$ and of order $\Delta(\phi \cdot \phi)$: as in the structural eigenproblems the eigenvector variation is typically larger than the corresponding eigenvalue one, then in Eq. 5 the corrective terms are of higher order with respect to $(\Delta \omega)$ and $(\Delta \omega)^2$ if $(\Delta \omega)$ represents the eigenfrequency variation. Nevertheless, this issue is true for a natural frequency variation and

not, for example, for an aerodynamic modification as it will be shown in the next Section.

Next, in order to perform the flutter analysis and the reversal-aileron analysis in term of state-space variables, let us introduce the finite-state approximation for the aerodynamics. The finite-state aerodynamic approximation for the GAF matrix introduced by Morino *et al.*,⁽²⁰⁾ yields

$$\tilde{\mathbf{f}}_m = \mathbf{E}(p)_m \tilde{\mathbf{q}} \simeq [\mathbf{E}_2 p^2 + \mathbf{E}_1 p + \mathbf{E}_0 + (\mathbf{I}p - \mathbf{P})^{-1} \mathbf{R}p] \tilde{\mathbf{q}} \quad (6)$$

where, for the sake of simplicity, only the aerodynamic matrix $\mathbf{E}_m(p)$ will be considered in the following. Considering the Eqs. 1, 3 and the finite state Aerodynamic approximation given by Eq. 6, the Lagrangian equations of motion in the Laplace domain become (with $\mathbf{E}_a(p) = 0$)

$$s^2 \mathbf{I} \tilde{\mathbf{q}} + \Omega^2 \tilde{\mathbf{q}} = q_D \left[\mathbf{E}_2 \frac{b^2}{U_\infty^2} s^2 + \mathbf{E}_1 \frac{b}{U_\infty} s + \mathbf{E}_0 + \left(\mathbf{I} \frac{b}{U_\infty} s - \mathbf{P} \right)^{-1} \mathbf{R} \frac{b}{U_\infty} s \right] \tilde{\mathbf{q}} \quad (7)$$

where the definition $p = sb/U_\infty$ has been used. Equation 7 can be rewritten as

$$\begin{cases} [\mathbf{M}_e s^2 + \mathbf{C}_e s + \mathbf{K}_e] \tilde{\mathbf{q}} + \tilde{\mathbf{r}} = 0 \\ \tilde{\mathbf{r}} = -q_D \left(\mathbf{I} \frac{b}{U_\infty} s - \mathbf{P} \right)^{-1} \mathbf{P} \mathbf{R} \tilde{\mathbf{q}} \end{cases} \quad (8)$$

where

$$\mathbf{M}_e := \mathbf{I} - q_D \mathbf{E}_2 \frac{b^2}{U_\infty^2} \quad (9)$$

$$\mathbf{C}_e := -q_D \mathbf{E}_1 \frac{b}{U_\infty} \quad (10)$$

$$\mathbf{K}_e := \Omega^2 - q_D \mathbf{E}_0 - q_D \mathbf{R} \quad (11)$$

are mass, damping, and stiffness equivalent matrices respectively. The above equation can be written in the time domain as

$$\begin{cases} \mathbf{M}_e \ddot{\mathbf{q}} + \mathbf{C}_e \dot{\mathbf{q}} + \mathbf{K}_e \mathbf{q} + \mathbf{r} = 0 \\ \dot{\mathbf{r}} - \frac{U_\infty}{b} \mathbf{P} \mathbf{r} = -q_D \frac{U_\infty}{b} \mathbf{P} \mathbf{R} \mathbf{q} \end{cases} \quad (12)$$

or in the normal form

$$\mathbf{B}(U_\infty, \alpha) \dot{\mathbf{x}} = \mathbf{A}(U_\infty, \alpha) \mathbf{x} \quad (13)$$

where $\mathbf{x}^T := \{\mathbf{q}^T | \dot{\mathbf{q}}^T | \mathbf{r}^T\}$, and

$$\mathbf{A}(U_\infty, \alpha) = \begin{bmatrix} 0 & \mathbf{I} & 0 \\ -\mathbf{K}_e & -\mathbf{C}_e & -\mathbf{I} \\ -q_D \frac{U_\infty}{b} \mathbf{P} \mathbf{R} & 0 & \frac{U_\infty}{b} \mathbf{P} \end{bmatrix} \quad (14)$$

$$\mathbf{B}(U_\infty, \alpha) = \begin{bmatrix} \mathbf{I} & 0 & 0 \\ 0 & \mathbf{M}_e & 0 \\ 0 & 0 & \mathbf{I} \end{bmatrix} \quad (15)$$

whereas α represents a structural-modification parameter in the geometrical, stiffness, or mass characteristics (when $\alpha = 0$, no structural modifications are considered) such that will modify the natural-frequency matrix Ω^2 , the mass matrix, and the GAF matrix $\mathbf{E}(p)$, *i.e.*, its approximating matrices \mathbf{E}_2 , \mathbf{E}_1 , \mathbf{E}_0 , \mathbf{P} , \mathbf{R} . Note that one could consider a vector of structural-modification parameters $\alpha^T := \{\alpha_1, \alpha_2, \dots\}$ but it does not change the following considerations and results.

Next, consider the presence of an aileron angle δ_c as a new Lagrangian variable associated to a suitable shape-mode function which is zero in all the wing domain and with a unit rotation for the aileron. Furthermore, consider also the rigid body motion around the roll axis and the associated lagrangian variable φ_x . Using the presented finite-state aerodynamics also for the aileron aerodynamic force $\tilde{\mathbf{f}}_a$ one can rewrite the Lagrange equations in the standard state-space form

$$\dot{\mathbf{x}} = \bar{\mathbf{A}} \mathbf{x} + \bar{\mathbf{B}} \delta_c \quad \dot{\varphi}_x = \bar{\mathbf{C}} \mathbf{x} \quad (16)$$

where the matrices $\bar{\mathbf{A}}$, $\bar{\mathbf{B}}$, and $\bar{\mathbf{C}}$ are the system matrix, the control matrix, and the output matrix of the aeroelastic system with input equal to aileron angle δ_c and output equal to the derivative with respect to time of the roll angle, $\dot{\varphi}_x$. The aileron reversal analysis can be carried out considering an input step function of $\delta_c(t)$ for a given velocity speed U_∞ : then, the aileron reversal happens when the $\dot{\varphi}_x$ assumes a negative value.

Aeroelastic Sensitivities

The method for the evaluation of the aeroelastic sensitivities presented in Balis Crema *et al.*⁽¹⁵⁾ is outlined in the following. Let us consider the eigenproblem associated to the Eq. 13

$$[\mathbf{A}(U_\infty, \alpha) - \lambda_n \mathbf{B}(U_\infty, \alpha)] \mathbf{u}^{(n)} = 0 \quad (17)$$

where $n = 1, 2, \dots, 3N$: indeed, the above eigenproblem can be solved for arbitrary values of the parameters U_∞ and α . Pre-multiplying Eq. 17 by the transposed of the left eigenvector $\mathbf{v}^{(n)T}$ (such as $\mathbf{v}^{(n)T} \mathbf{u}^{(n)} = 1$ (*i.e.*, $\mathbf{V}^T = \mathbf{U}^{-1}$, where \mathbf{V} and \mathbf{U} are the left and right eigenvectors matrix respectively) one has for all eigenvalues (eigenvectors):

$$\mathbf{v}^{(n)T} [\mathbf{A}(U_\infty, \alpha) - \lambda_n \mathbf{B}(U_\infty, \alpha)] \mathbf{u}^{(n)} = 0 \quad (18)$$

In order to obtain the derivative of the flutter speed and the frequency speed with respect to α ($U_{F,\alpha}$ and $e \lambda_{F,\alpha}$), let us derive Eq. 18 with respect to α (for the sake of simplicity, we shall not indicate in the following the dependence on U_∞ and α)

$$\frac{\partial \mathbf{v}^{(n)T}}{\partial \alpha} [\mathbf{A} - \lambda_n \mathbf{B}] \mathbf{u}^{(n)} \quad (19)$$

$$+\mathbf{v}^T [\mathbf{A} - \lambda_n \mathbf{B}] \frac{\partial \mathbf{u}^{(n)}}{\partial \alpha} + \mathbf{v}^{(n)T} \left[\frac{\partial \mathbf{A}}{\partial U} U_{,\alpha} + \frac{\partial \mathbf{A}}{\partial \alpha} - \lambda_n \left(\frac{\partial \mathbf{B}}{\partial U} U_{,\alpha} + \frac{\partial \mathbf{B}}{\partial \alpha} \right) - \frac{d\lambda_n}{d\alpha} \mathbf{B} \right] \mathbf{u}^{(n)} = 0$$

Reordering the above equation with respect to the unknowns $U_{,\alpha} := \partial U / \partial \alpha$ and $d\lambda_n / d\alpha$ yields

$$\mathbf{v}^{(n)T} \left[\frac{\partial \mathbf{A}}{\partial U} - \lambda_n \frac{\partial \mathbf{B}}{\partial U} \right] \mathbf{u}^{(n)} U_{,\alpha} - \mathbf{v}^{(n)T} \mathbf{B} \mathbf{u}^{(n)} \frac{d\lambda_n}{d\alpha} = -\mathbf{v}^{(n)T} \left(\frac{\partial \mathbf{A}}{\partial \alpha} - \lambda_n \frac{\partial \mathbf{B}}{\partial \alpha} \right) \mathbf{u}^{(n)} \quad (20)$$

In the flutter condition, for all the α 's, one has a characteristic flutter velocity $U_{\infty F}(\alpha)$ such as the corresponding critical eigenvalues $\lambda_F(\alpha)$ has $Re[\lambda_F(\alpha)] = 0$. When the Eq. 20 is written correspondingly to the flutter condition ($\lambda_n = j\omega_F$, $\mathbf{u}^{(n)} = \mathbf{u}_F$ e $\mathbf{v}^{(n)} = \mathbf{v}_F$), one has

$$\mathbf{v}_F^T \left[\frac{\partial \mathbf{A}}{\partial U} - j\omega_F \frac{\partial \mathbf{B}}{\partial U} \right] \mathbf{u}_F U_{,\alpha} - j\mathbf{v}_F^T \mathbf{B} \mathbf{u}_F \frac{d\omega_F}{d\alpha} = -\mathbf{v}_F^T \left(\frac{\partial \mathbf{A}}{\partial \alpha} - j\omega_F \frac{\partial \mathbf{B}}{\partial \alpha} \right) \mathbf{u}_F \quad (21)$$

The equation 21 can be rewritten as

$$a U_{,\alpha} + b \frac{d\omega_F}{d\alpha} = c \quad (22)$$

i.e., considering the real and the imaginary parts,

$$a_R U_{,\alpha} + b_R \frac{d\omega_F}{d\alpha} = c_R \quad (23)$$

$$a_I U_{,\alpha} + b_I \frac{d\omega_F}{d\alpha} = c_I \quad (24)$$

The above linear system gives the two flutter derivatives with respect to the structural modification α . Note that in order to solve the above eigensensitivity problem, one needs the derivative $\partial \mathbf{A} / \partial U_{\infty}$, $\partial \mathbf{B} / \partial U_{\infty}$, $\partial \mathbf{A} / \partial \alpha$, and $\partial \mathbf{B} / \partial \alpha$: considering the Eqs. 9, 10, 11, 14, and 15, one explicitly obtains

$$\frac{\partial \mathbf{A}}{\partial U_{\infty}} = \begin{bmatrix} 0 & 0 & 0 \\ \rho U_{\infty} (\mathbf{E}_0 + \mathbf{R}) & \frac{1}{2} \rho \mathbf{E}_1 b & 0 \\ -\frac{3}{2} \rho \frac{U_{\infty}^2}{b} \mathbf{P} \mathbf{R} & 0 & \frac{\mathbf{P}}{b} \end{bmatrix}$$

$$\frac{\partial \mathbf{B}}{\partial U_{\infty}} = \begin{bmatrix} 0 & 0 & 0 \\ 0 & 0 & 0 \\ 0 & 0 & 0 \end{bmatrix} = \mathbf{0}$$

$$\frac{\partial \mathbf{A}}{\partial \alpha} = \begin{bmatrix} 0 & 0 & 0 \\ q_D \mathbf{E}_{0,\alpha} + q_D \mathbf{R}_{,\alpha} - \Omega_{,\alpha}^2 & q_D \frac{U_{\infty}}{b} \mathbf{E}_{1,\alpha} & 0 \\ -q_D \frac{U_{\infty}}{b} (\mathbf{P}_{,\alpha} \mathbf{R} + \mathbf{P} \mathbf{R}_{,\alpha}) & 0 & \frac{U_{\infty}}{b} \mathbf{P}_{,\alpha} \end{bmatrix}$$

$$\frac{\partial \mathbf{B}}{\partial \alpha} = \begin{bmatrix} 0 & 0 & 0 \\ 0 & -q_D \frac{b^2}{U_{\infty}^2} \mathbf{E}_{2,\alpha} & 0 \\ 0 & 0 & 0 \end{bmatrix}$$

Note that the variations $\mathbf{E}_{0,\alpha}$, $\mathbf{E}_{1,\alpha}$, $\mathbf{P}_{,\alpha}$, $\mathbf{R}_{,\alpha}$ are higher order terms with respect to α – because they

are all dependent on the modal shapes – if one does not consider shape variations, Balis Crema et al. ⁽¹⁵⁾: in this case one can take into account the following simplified expressions:

$$\frac{\partial \mathbf{A}}{\partial \alpha} \cong \begin{bmatrix} 0 & 0 & 0 \\ -\Omega_{,\alpha}^2 & 0 & 0 \\ 0 & 0 & 0 \end{bmatrix}; \quad \frac{\partial \mathbf{B}}{\partial \alpha} \cong \mathbf{0} \quad (25)$$

Numerical Results

In the present Section some numerical results on a *UHCA* wing-body configuration will be presented: all the data are provided by CIRA and some general characteristics of the airplane are presented in Tab. I and the wing shape with a typical aerodynamic mesh considered in the computation is shown in Fig. 1. The stiffness characteristics given by the $EI(y)$ and $GJ(y)$ curves are depicted in Fig. 2: considering these informations, a finite element model with around 100 d.o.f.s has been implemented using the *MSC – NASTRAN* code (*CBEAM* elements and three-mass chord-wise distribution have been taken into account).

Wing Surface	745	m^2
Wing Span	78	m
Chord at Wing Root	16.147	m
Chord at Wing Tip	3.505	m
Mean Chord	11.367	m
Maximum Take-off Weight (<i>MTOW</i>)	550000	Kg
Operative Empty Weight (<i>OEW</i>)	271900	Kg
Wing (structural) Weight	88477	Kg
Max Payload	77600	Kg
Fuel Weight	200500	Kg
Engine-pylon Weight	7000	Kg
U_D	215	m/s

Tab. 1: *UHCA* characteristics

The modal analysis of the structure with fuel, with first ten eigenfrequencies reported in Tab. II, shows that out-of-plane torsional (T), bending (B), in-plane bending (B*), and coupled (B/T) modes are present in the range of eigenfrequencies considered. Note that the second mode is a bending/torsional mode that is essentially influenced by the presence of the engines. The engine locations are at 13.015 m and 22.915 m from the wing root, the nacelle axis is 2.3 m distant from the wing lifting surface, and nacelle leading edge is around 5 m distant from the wing leading edge: the nacelle diameter is 3.5 m and its length is 5 m . Note that the aerodynamic influence given by the nacelle is not due to the engine-trust forces (which are practically constant and then they do not influence the stability) but only by the unsteady aerodynamic loads

due to the nacelle elastic motion (*i.e.*, a ring-wing behavior is taken into account).

The flight conditions considered in the aeroelastic test are a Mach number $M_\infty = 0.8$ and an altitude corresponding to a standard air density $\rho = 1.22 \text{ kg/m}^3$. The GAF matrix has been obtained with a doublet-lattice method, Albano ⁽¹⁸⁾, by the *MSC - NASTRAN* code: the aerodynamic mesh considered is: 10 panels chord-wise, 20 span-wise, 10 panels streamwise on the engine-nacelle and 9 panels around it. The number of GAF matrix evaluation is equal to 16 in a range of the reduced frequency $0 < k < 0.8$. In Figure 3 the root locus for $10 < U_\infty < 280$ corresponding to the above reference aeroelastic configuration is shown: note that the critical mode (avoiding the contribution of the rigid mode) is the first one with flutter speed $U_F = 272.82 \text{ m/s}$ and a flutter frequency $f_F = 1.20 \text{ Hz}$: this result is in agreement with that predicted by Försching ⁽¹⁾ in the sense that a typical engine-nacelle pitch flutter occurs.

n	Freq. (Hz)	Mode Type
1	0.	Plunge mode
2	0.470	B
3	1.415	B/T
4	2.351	T
5	3.330	T
6	3.994	B*/T
7	4.167	B*
8	5.482	B/T
9	6.161	B/T
10	8.913	B/T

Tab.II: *UHCA* Modal analysis

Next, let us consider the aileron-reversal analysis. For several values of the air speed U the steady value $\dot{\varphi}_x^C$ of the response φ_x after a step input for the aileron angle δ_c has been evaluated: the resulting steady values, normalized with respect to the response $\dot{\varphi}_{xR}^C$ obtained in the hypothesis of rigid body motion (as well known, in this case the response is air speed independent), are depicted in Fig. 4. Note that the reversal-aileron critical speed U_{ar} , which is about 200 m/s , is theoretically inside the flight envelope ($U_{ar} < U_D$): this is probably due to position of the aileron at the extreme tip of the wing; however, as suggested by Försching ^(1, 2, 3), the action of leading edge surfaces, *e.g.*, slats, should improve this aeroelastic behavior.

Finally, the results on the aeroelastic sensitivity analysis. First, let us consider variations of global characteristics of the wing such as the stiffness distribution and fuel mass distribution. In Figure 5 the flutter speed is depicted as function of a global reduction in bending stiffness (EI) with constant torsional stiffness, torsional stiffness (GJ) with constant bend-

ing stiffness, and, finally, both torsional and bending stiffness keeping constant the stiffness ratio: note that these are global reductions in the sense that the shape of the stiffness distribution is that depicted in the Fig. 2. These curves are obtained neglecting the influence of the engine nacelle and considering the presence of the fuel. In the same Figure there are also the straight lines tangent in three different points of the curves and obtained with the sensitivity analysis presented above considering only the stiffness variations in the sensitivity matrices. Note that the most influential contribution in the flutter speed decrease is given by the torsional stiffness. In Figure 6 the sensitivity to the fuel-mass variation (0=empty, 1=full) is estimated considering the presence or not of the aerodynamic influence of the engine nacelle: the presence of the nacelles decreases the flutter speed; furthermore, as in the previous Figure, the tangent lines obtained with the sensitive analysis are also depicted as obtained by the variation of the (unit) mass matrix.

Next, in Figs. 7 and 8 the influence of the engine weight in presence and in absence of fuel respectively, is analyzed: the curves considering the influence of the nacelle are always lower with respect to the other; moreover, the good influence of the engine weight for the flutter stability is evident in absence of fuel; again, the tangent lines are obtained as shown in the previous Figure.

In Figure 9 and 10 the influence of the engines stream-wise locations in presence and in absence of fuel respectively is considered: the influence of this parameter is relevant above all in absence of fuel and in presence of the effects due to the nacelles. However, the global effect of the presence of the nacelles is the same found in the previous cases. Note that the estimates of the flutter derivative are obtained also in this case considering only the mass matrix variations (*i.e.*, $\partial \mathbf{I} / \partial \alpha$) and avoiding the aerodynamic matrices variations.

In Figures 11 the influence of the engine vertical position is analyzed in absence of fuel (no estimable variations have been found in presence of fuel): the flutter speed increases very regularly with the vertical displacement (when it is allowed by the physical constraints) and then the tangent lines are practically coincident with the curves. Moreover, the presence of the nacelle decreases the flutter speed.

Finally, the Figure 12 depicts the flutter speed variation as function of the ratio between the nacelle diameter and the nacelle length (D/L): the variation due to this parameter is almost linear and then the estimate given by the sensitivity is quite good. Note that in this case the aeroelastic sensitivities are evaluated considering necessarily the variations of the aerodynamic matrices. The presence of the fuel seems to reduce this destabilizing effects due to D/L ratio. he significant

Concluding Remarks

In the present paper the influence of several structural modifications as the global stiffness, the fuel mass, the mass, position and dimension of the engine, on the aeroelastic analysis of a *UHCA* has been investigated. This analysis is based on a finite-state aerodynamic modeling and on the estimates of the mass, stiffness and aerodynamic variations and for every cases considered in the analysis a good estimation of such sensitivities has been carried. Specifically:

- a low frequency flutter occurs because of the coupling between the first bending mode and the second torsional/bending mode;
- in all the cases considered, the presence of the fuel generally reduce the flutter velocity;
- in all the cases considered, the influence of the nacelle airload typically decreases the flutter speed;
- the nacelle displacement in streamwise direction and the nacelle diameter influence considerably the flutter speed;

Moreover, the aeroelastic analysis on the aileron effectiveness of this kind of wing exhibits that the aileron revers may occurs before the velocity U_D , *i.e.*, within the flight envelope.

Acknowledgement

This work has been supported by the Ministero dell'Università e della Ricerca Scientifica e Tecnologica, grant 1993/94: "Modellazione computazionale di problemi aeroservoelastici".

References

1. Försching, H., "The Impact of Aeroelasticity on the Design of New Ultra High Capacity Aircraft (UHCA)," Festschrift in honor of Prof. P. Santini, 1993, pp. 7-32.
2. Försching, H., "Challenges and Perspectives in Computational Aeroelasticity," Proceedings of *International Forum on Aeroelasticity and Structural Dynamics*, Manchester, U.K., 26-28 June, 1995, Royal Aeronautical Society, pp. 1.1-1.9.
3. Försching, H., Knaack, J.M., "Engine Nacelle Model in Subsonic Flow," *Journal of Fluids and Structures*, 1993, pp. 567-593.
4. Bisplinghoff, R. L., Ashley, H., and Halfman, R. L., *Aeroelasticity*, Addison-Wesley, Reading, MA, 1955.
5. Haftka, R.T., Gurdal, E.Z., *Elements of Structural Optimization*, Kluwer, 1992.

6. Haftka, R.T., Yates, E.C., "Repetitive Flutter Calculation in Structural Design," *Journal of Aircraft*, Vol. 13, No. 7, July 1976, pp.454-461.
7. Striz, A.G., Venkayya, V.B., "Influence of Structural and Aerodynamic Modeling on Flutter Analysis," *AIAA Journal*, Vol. 31, No. 5, Sept.-Oct. 1994, pp. 1205-1211.
8. Cardani, C., Mantegazza, P., "Calculation of Eigenvalue and Eigenvector Derivatives for Algebraic Flutter and Divergence Eigenproblems," *AIAA Journal*, Vol. 17, No. 4, April 1979, pp.408-412.
9. Rogers, L.C., "Derivative of Eigenvalues and Eigenvectors," *AIAA Journal*, Vol. 8, No. 5, May 1970, pp. 943-944.
10. Jones, R. T., "The Unsteady Lift of a Wing of Finite Aspect Ratio," NACA 681, 1940.
11. Karpel, M., "Design for the Active Flutter Suppression and Gust Alleviation Using State-Space Aeroelastic Modeling," *Journal of Aircraft*, Vol. 19, March 1982, pp. 221-227.
12. Morino, L., Mastroddi, F., De Troia, R., Ghiringhelli, G. L., Mantegazza, P., "Matrix Fraction Approach for Finite-State Aerodynamic Modeling," *AIAA Journal*, Vol. 33, No. 4, April 1995, pp. 703-711.
13. Karpel, M., "Sensitivity Derivatives of Flutter Characteristics and Stability Margins for Aeroservoelastic Design," *AIAA Journal*, Vol. 27, No. 4, April 1990, pp. 368-375.
14. Karpel, M., Brainin, L., "Stress Considerations in Reduced-Size Aeroelastic Optimization," *AIAA Journal*, Vol. 33, No.4, April, 1995, pp. 716-722.
15. Balis Crema, L., Mastroddi, F., Coppotelli, G., "Structural Modeling Effects on Aeroelastic Analysis," Proceedings of *International Forum on Aeroelasticity and Structural Dynamics*, Manchester, U.K., 26-28 June, 1995, Royal Aeronautical Society, pp. 40.1-40.11.
16. Morino, L., "A General Theory of Unsteady Compressible Potential Aerodynamics," NASA CR-2464, Dec. 1974.
17. Morino, L., "Boundary integral equations in aerodynamics," *Applied Mechanical Reviews*, Vol. 46, No. 8, Aug. 1993, pp. 445-466.
18. Albano, E., and Rodden, W.P., "A doublet Lattice Method for Calculating Lift Distributions on Oscillating Surfaces in Subsonic Flos," *AIAA Journal*, Vol. 7, pp. 279-285, p. 2192.
19. Giesing, J.P., Kalman, T.P., and Rodden, W.P., "Subsonic Steady and Oscillatory Aerodynamics for Multiple Interfering Wings and Bodies," *Journal of Aircraft*, Vol. 9, pp. 693-702.

20. Morino, L., Mastroddi, F., De Troia, R., and Pecora, M., "On the Modeling of Aeroservoelastic Problems," *Proceedings of the International Forum on Aeroelasticity and Structural Dynamics*, Strasbourg, France, May 1993, pp. 97-116.
21. Morino, L., (Ed.) *Computational Methods in Potential Aerodynamics*, Computational Mechanics Publications, Southampton, U.K., 1985.
22. Morino, L., "Steady, Oscillatory, and Unsteady Subsonic and Supersonic Aerodynamics," *Productions Version (SOUSSA-P 1.1) - Vol. 1, theoretical manual*, NASA CR 159130, Jan. 1980.

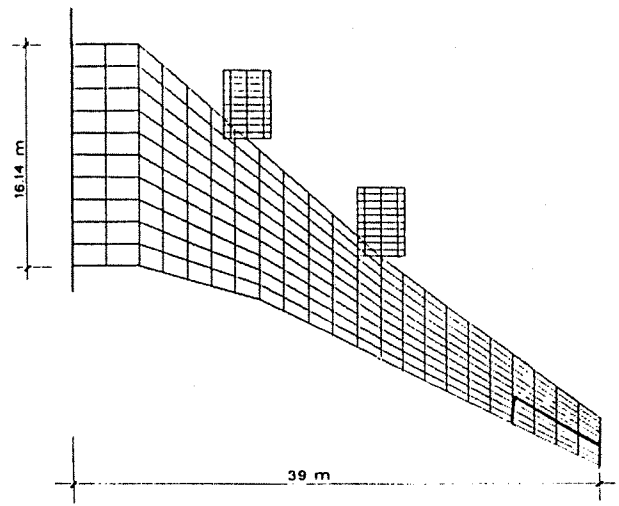


Figure 1:

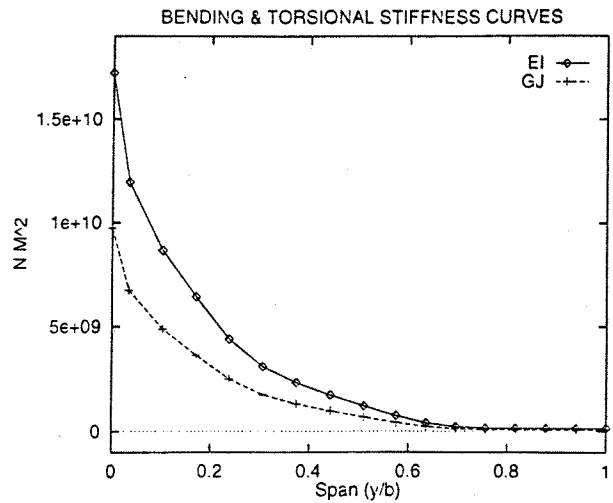


Figure 2:

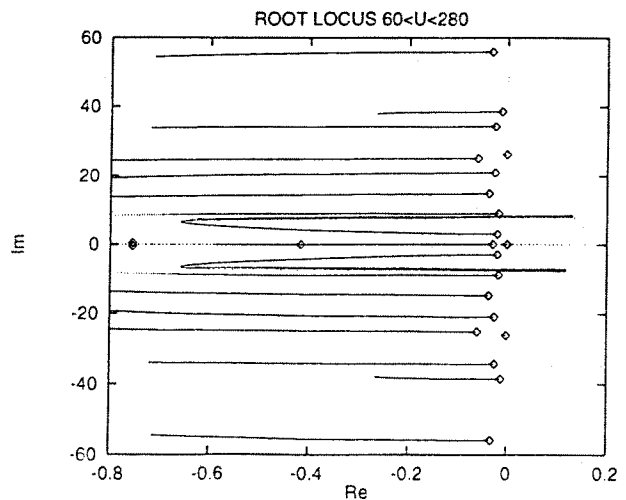


Figure 3:

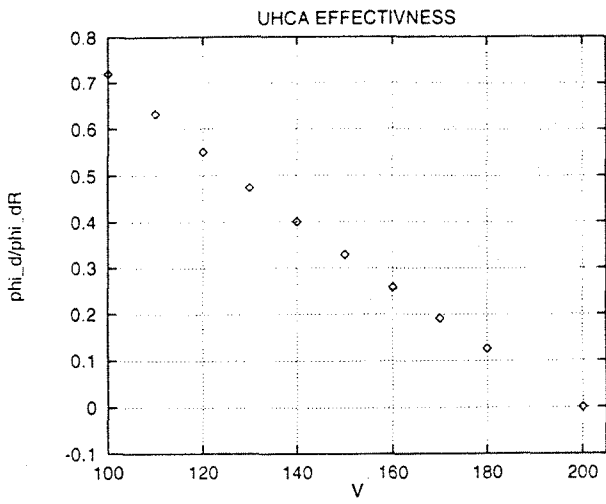


Figure 4:

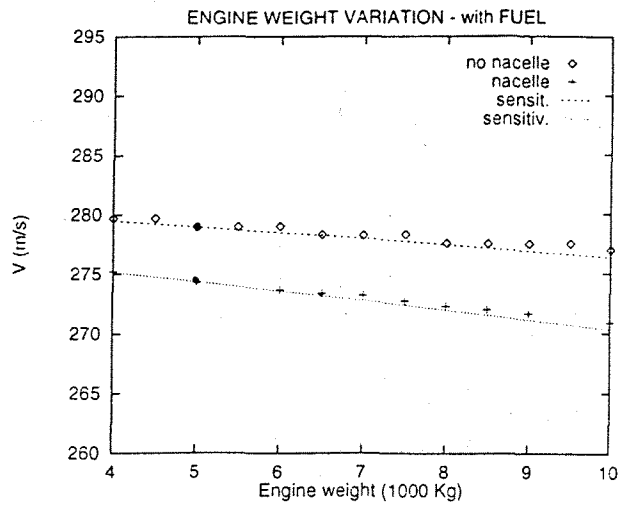


Figure 7:

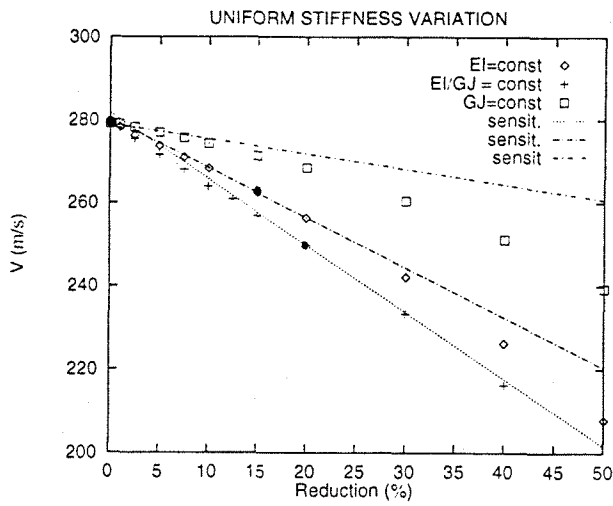


Figure 5:

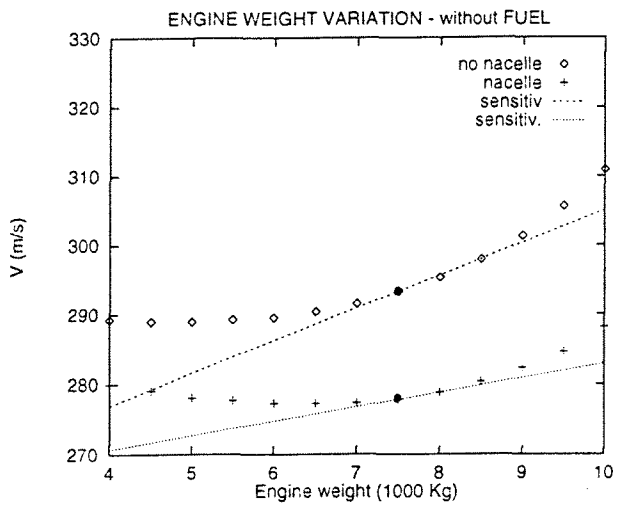


Figure 8:

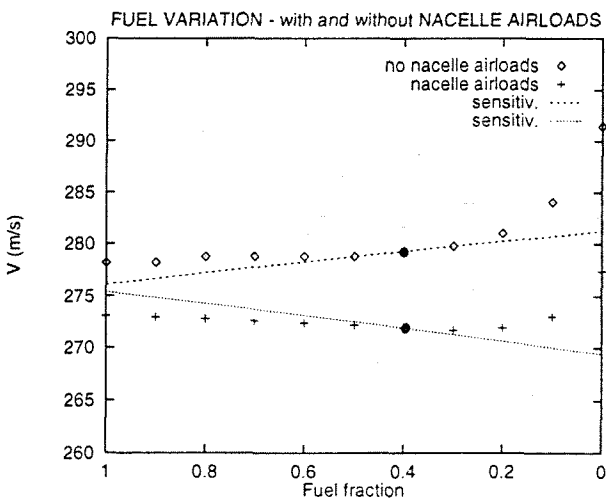


Figure 6:

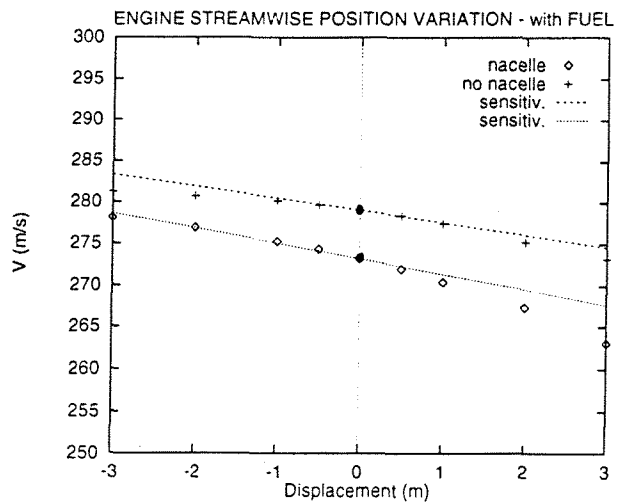


Figure 9:

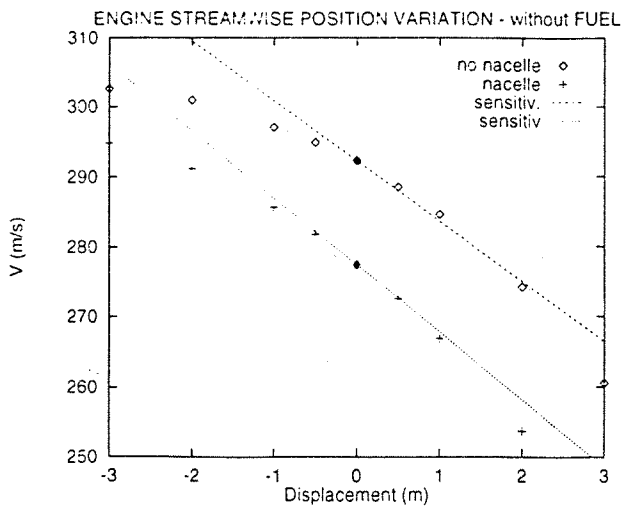


Figure 10:

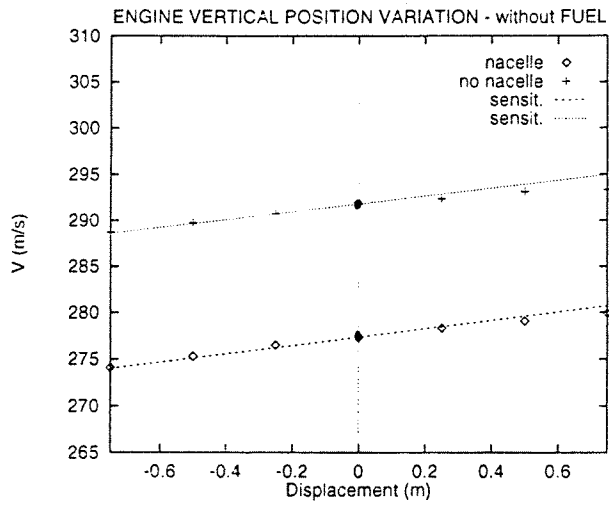


Figure 11:

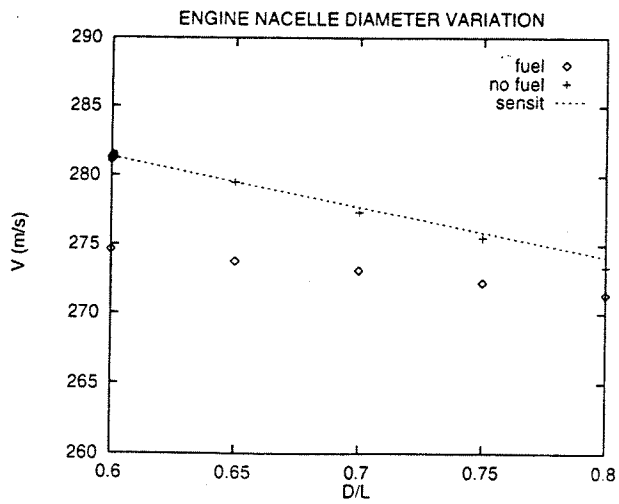


Figure 12: